

Studies on the Fe-P Film Plating from a Chemical Bath: Deposition Mechanism and Parameter Effects

Gui-Fang Huang^{1,*}, Wei-Qing Huang¹, Ling-Ling Wang¹, Bing-Suo Zou¹, Qiao-Ling Wang², Jian-Hui Zhang²

¹ College of Physics and Microelectronics, Hunan University, Changsha 410082, China

² Changsha Environmental Protection College, Changsha 410004, PR China

*E-mail: gfhuang@hnu.cn

Received: 3 November 2007 / Accepted: 22 November 2007 / Online published: 20 December 2007

Electroless Fe-P film was prepared from a chemical bath by connecting an aluminum foil to the brass substrate during deposition. The deposition mechanism of electroless Fe-P film was discussed and proposed. It is found that, due to the Al dissolution, the Fe film firstly deposited on the substrate keeps the substrate surface active, thus assures the chemical reduction of iron ions by hypophosphite continuously during the whole deposition process. The Fe-P film results from a superimposition of the electrochemical process due to the galvanic cell with Fe film deposition and Al dissolution and the chemical process due to the reduction of the Fe cations by H_2PO_2^- anions, accompanied by phosphorus co-deposition. We also investigated the effects of bath component and process parameters on the electroless Fe-P deposition. The results show that the bath component and process parameters obviously effect the formation and the composition of Fe-P film. The effect of hypophosphite on the deposition rate is more pronounced than that of FeSO_4 due to the higher polarization resistance of anodic reaction, indicating that the rate-determining step for the chemical iron reduction is the oxidation of hypophosphite. The understanding of Fe-P deposition mechanism is beneficial for development of new electroless Fe-based alloy films.

Keywords: Deposition mechanism, Electroless deposition, Fe-P Film

1. INTRODUCTION

Electroless deposition process has been extensively studied and widely applied in varied areas due to its industrial importance, featuring its capability to form uniform films with excellent behaviors on various substrates [1-12]. It is widely accepted that electroless deposition proceeds along the electrochemical mechanism as a simultaneous reaction of cathodic metal deposition and anodic oxidation of a reductant at the same catalytically surface[13]. The electron for reductive deposition of

metal species is supplied by catalytic oxidation reaction of reductant molecules in the bath instead of by the external current. To establish basic mechanism of the electroless deposition, a great deal of research has been carried out to elucidate the anodic and the cathodic processes using electrochemical and kinetic methods [14-16]. The deposition mechanisms of electroless Ni, Co, Cu alloys films have been investigated and several reaction paths were proposed [13, 17-20]. However, to the best of our knowledge, the deposition mechanism of electroless Fe-P films is still insufficient. Electroless Fe-P films were first obtained by Ruscior[21] and the substrates are usually connected with an aluminium foil during iron alloys deposition [21-28]. This deposition method raises the question of the mechanism of electroless iron alloys deposition.

This work investigated the deposition mechanism of Fe-P film plating from a chemical bath. The influences of various experimental parameters, such as hypophosphite and iron sulphate concentrations, bath pH and temperature, on the deposition rate were studied by gravimetric method. The reactions for electroless Fe-P deposition were developed and discussed. The reaction orders of bath ingredients were determined by plotting the logarithm of deposition rate versus the logarithm of concentration of metal salt, reducing agent, and hydrogen ion, respectively, and the activation energy was also determined by plotting the logarithm of deposition rate versus reciprocal of temperature.

2. EXPERIMENTAL PART

The Fe-P film was prepared on brass substrate by electroless plating from a sulphate bath. The brass foil (25×15×2 mm) and brass electrode ($\phi = 20$ mm) embedded in an epoxy resin were used as substrates. The bath was prepared with analytical grade reagents dissolved in de-ionized water. The bath composition and process parameters are shown in Table 1. The pH was adjusted using 15wt% NaOH solution and measured by electronic pH-meter Orion model 720A. During deposition, the substrate was connected with aluminum foil through a copper wire. To perform the gravimetric measurement, the weights of samples before and after deposition were determined by electronic microbalance model HT-300, and the plating rate, $w(\mu\text{m}/\text{h})$, can be calculated from the weight difference before and after deposition and the assumption density of $7.8\text{g}/\text{cm}^3$ for the film obtained.

Table 1. Chemical composition (mM) and operating conditions of the electroless plating bath

solution	FeSO ₄ ·7H ₂ O	NaH ₂ PO ₂ ·H ₂ O	KNaC ₄ H ₄ O ₆ ·4H ₂ O	H ₃ BO ₃	C ₁₂ H ₁₂ O ₁₁
oxidation	59	-	128	48.5	3.6
reduction	-	170	128	48.5	3.6
plating	20~79	57~284	128	48.5	3.6
pH	8~11.5		T	50~85°C	

The electrochemical measurement was carried out with a three-compartment cell using the electrochemical analyzer CHI-660B. A platinum foil with size 20×40 mm² was used as an auxiliary electrode and a saturated calomel electrode was used as reference electrode. The working electrode was the brass electrode connected with aluminum foil. The potential of electrode was measured vs.

saturated calomel electrode with time. In order to simulate partial cathodic or anodic reaction, the investigation of the electrolytes in the absence of either the $\text{Na}_2\text{H}_2\text{PO}_2$ reductant(oxidation solution) or the FeSO_4 (reducing solution) was carried out. The compositions of the films were evaluated using scanning electron microscopy (SEM, JEOL JSM-5600LV) combined with energy dispersive spectrometry (EDS).

3. RESULTS AND DISCUSSION

3.1. Elementary reaction pathways

Experiment shows that no film forms on the brass substrate in bath unless the substrate is connected with aluminum, indicating that it is necessary for brass substrate to be connected with aluminum for electroless Fe-P(B) deposition [21-28]. In a previous work we explored the inducing mechanism of the connected aluminum on Fe-P electroless deposition[29]. It was shown that the connected aluminum induces Fe-P electroless deposition. Due to the galvanic cell composed of brass and aluminum in the chemical bath, iron film forms on the brass substrate, which raised the question of the mechanism of Fe-P electroless deposition.

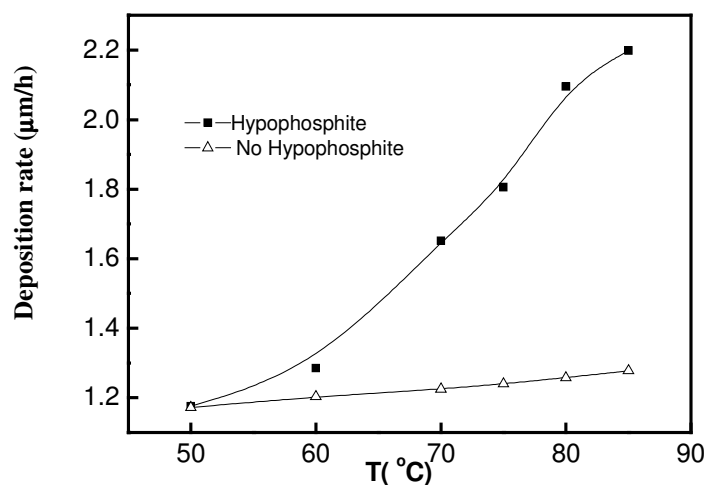
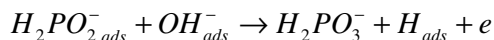


Figure 1. The deposition rates in bath containing hypophosphite and in the bath without hypophosphite

To investigate the reaction pathway for Fe-P deposition, the deposition rates of the film obtained from the bath with and without hypophosphite under the same conditions were measured. As shown in Fig.1, the deposition rate of film increases with bath temperatures ranging from 50 to 85 °C. However, the deposition rate in the bath without hypophosphite increases almost linearly with temperature, while the deposition rate in the bath with hypophosphite increases sharply with temperature when the bath temperature is higher than 60 °C. The deposition rate in the bath with and without hypophosphite is almost the same as the bath temperature is 50 °C. Whereas, the deposition rate in the bath containing hypophosphite is obviously higher than that in the bath without

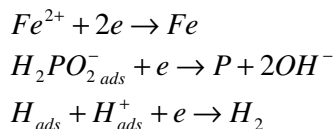
hypophosphite when the bath temperature is higher than 60 °C. The deposition rate in the bath with hypophosphite is almost twice of that in the bath without hypophosphite as bath temperature reaches 80 °C. The energy spectrum results show that the film obtained from the bath without hypophosphite is a pure iron layer, while those obtained from the bath with hypophosphite are Fe-P alloy and the content of phosphorus depends on bath temperature and pH (For example, the film deposited at 80 °C and pH=10.5 contain 5.53 at% P and 94.47 at% Fe). The formation of the pure iron film, originating from the reduction of iron cations by currents arising from the galvanic cell composed of the brass substrate as cathode and the connected aluminum foil as anode, provides a catalytic surface for the Fe-P electroless deposition. The hypophosphite adsorbed on the catalytic surface, followed by its reorientation and oxidation. The electrons released by the oxidation of $H_2PO_2^-_{ads}$ would be gained by the iron ions and/or $H_2PO_2^-_{ads}$, thus lead to the electroless Fe-P deposition. The difference between the deposition rates in two baths with and without hypophosphite under the same conditions can be attributed to the Fe-P deposition, i.e., only Fe film formed due to the Al dissolution and Fe cation reduction in the bath without hypophosphite, while Fe-P film formed in the bath with hypophosphite due to the reduction of the Fe cations by $H_2PO_2^-$ anions and the Al dissolution, accompanied by phosphorus co-deposition.

From the above results, it can be concluded that the Fe-P deposition arises from a superimposition of the electrochemical process formed the Fe film due to the Al dissolution and the chemical process due to the reduction of the Fe cations by $H_2PO_2^-_{ads}$ anions, accompanied by phosphorus co-deposition and hydrogen evolution. The connected Al during the process keeps the substrate surface active, and provides the necessary catalyst for the chemical reduction of iron ions by hypophosphite. With bath temperature increasing, the chemical process enhances, the difference between the deposition rates in two baths with and without hypophosphite under the same conditions increases. The electroless deposition using hypophosphite as a reducer can be divided into two processes: anodic and cathodic reactions. The anodic reaction is the oxidation of $H_2PO_2^-_{ads}$ on the catalytic surface. It can be described as

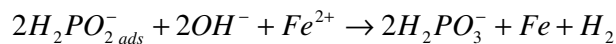


At the same time, the released electrons take part in the cathodic reactions.

The cathodic reactions are: (1) reduction of iron ions, (2) reduction of hypophosphite, and reduction of hydrogen ions. These procedures can be given as follows:



Then, the chemical reaction for Fe deposition reduced by hypophosphite can be expressed as following:



The general form of the deposition rate can be written as follows:

$$v = dFe / dt = k[H_2PO_2^-]^\alpha [Fe^{2+}]^\beta [OH^-]^\gamma [H_2PO_3^-]^\varepsilon \exp(-E_a / RT)$$

where v is the deposition rate ($\mu m/h$), T is the temperature (K), and E_a is activation energy.

Then

$$\text{Log} v = k_1 + \alpha \text{Log}[H_2PO_2^-] + \beta \text{Log}[Fe^{2+}] + \gamma \text{pH} + \varepsilon \text{Log}[H_2PO_3^-] - E_a / RT$$

In which

$$\alpha = d\text{Log} v / d\text{Log}[H_2PO_2^-]$$

$$\beta = d\text{Log} v / d\text{Log}[Fe^{2+}]$$

$$\gamma = d\text{Log} v / \text{pH}$$

$$\varepsilon = d\text{Log} v / d\text{Log}[H_2PO_3^-]$$

are the reaction orders of $H_2PO_2^-$, Fe^{2+} , H^+ , and $H_2PO_3^-$, respectively.

3.2. The effects of deposition parameters on the deposition rate

Fig.2 (a) shows the effect of $FeSO_4$ concentration on the deposition rate. It is clear that the deposition rate increases, then, decreases after a maximum with the increase of $FeSO_4$ concentration. The change can be interpreted as follows. On the one hand, $FeSO_4$ is the provider for iron deposition, and an increase of $FeSO_4$ concentration increases the free iron ions available for reduction, resulting in an increase in deposition. On the other hand, the further increase of the concentration of the free iron ions may lead the formation of hydroxid and phosphide of iron, which acts as catalyzing center where iron ions may be reduced, thus the iron ions reduced on the substrate decrease, i.e., the deposition rate decreases. The data where the deposition rate increase with the concentration of iron sulfate are used to plot the logarithm of deposition rate as a function of logarithm of iron sulfate concentration in Fig.2(b) the slope of which is the reaction order β .

Sodium hypophosphite is the reductant, the oxidation of hypophosphite anions releases the electrons needed to reduce iron ions and hypophosphite for Fe-P film deposition. Therefore the deposition rate is expected to increase with the increase of the sodium hypophosphite concentration. The maximum of deposition rate maybe result from the formation of phosphide of iron. The data where the deposition rate increases with the concentration of sodium hypophosphite are used to plot the logarithm of deposition rate as a function of logarithm of sodium hypophosphite concentration in Fig.3(b), the slope of which is the value.

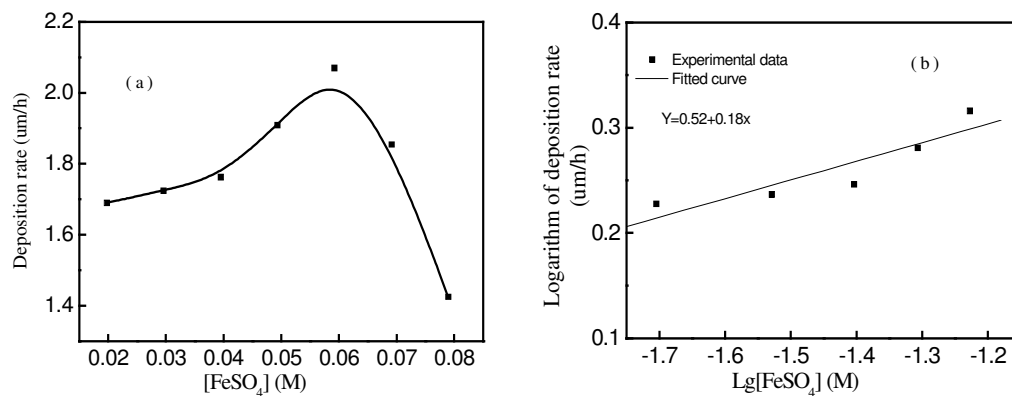


Figure 2. (a) Effect of ferrous sulfate concentration on deposition rate, (b) Plot of logarithm of deposition rate versus logarithm of ferrous sulfate concentration

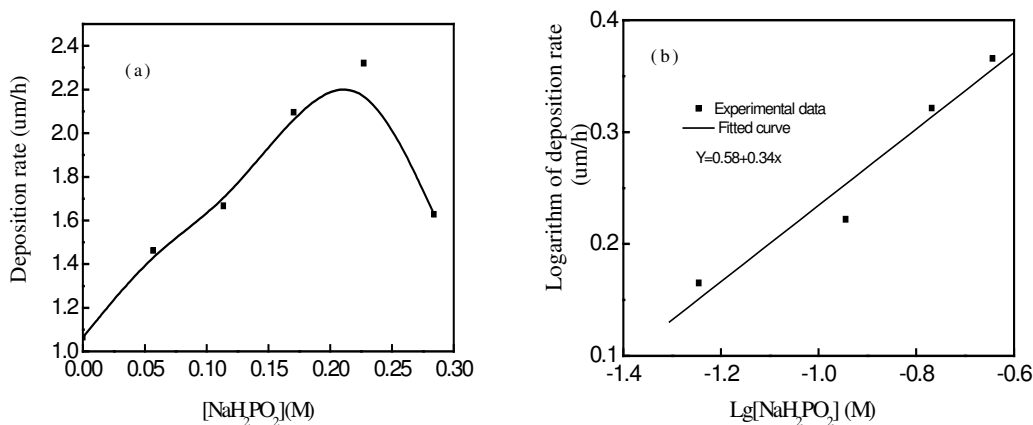


Figure 3. (a) Effect of sodium hypophosphite concentration on deposition rate (b) Plot of logarithm of deposition rate versus logarithm of sodium hypophosphite

The pH has significant influence on the deposition process and the deposition rate. Fig.4 (a) illustrates the effect of bath pH on the deposition rate. One can see from Fig.4(a) that the deposition rate increases first, and decreases after reaching a maximum deposition rate with the bath pH increase. Experiment showed that there is few deposit on the substrate as the bath pH lower than 8, while the bath solution appeared turbid during deposition as the bath pH higher than 11.5. The deposition reactions suggest that the oxidation of $H_2PO_2^-$ is difficult to take place as the pH of plating bath is too low. With the increase of the pH of plating bath, i.e., the increase of the concentration of hydroxy ions in bath, facilitates the oxidation of $H_2PO_2^-$, thus increases the deposition rate. However, with the further increase of the bath pH, the concentration of hydroxyl ions in bath increases, leading to the formation of $Fe(OH)_2$ colloid, which can acted as catalytically center where Fe-P deposition occurs, therefore, the bath become instability and the deposition rate decreases. The data where the deposition rate increase with the pH are used to plot the logarithm of deposition rate as a function of logarithm of

hydrogen ions concentration in Fig.4 (b), the slope of which is the γ value. The $H_2PO_3^-$ ion is the byproduct of the electroless Fe-P deposition which accumulates in the solution and its effect on deposition rate may be ignored. Therefore, ε may be set a value of 0. According to Figs. 2 (b)-4 (b), we calculated the reaction orders of NaH_2PO_2 , $FeSO_4$ and H^+ : $\alpha = 0.34$, $\beta = 0.18$, $\gamma = 0.13$, respectively.

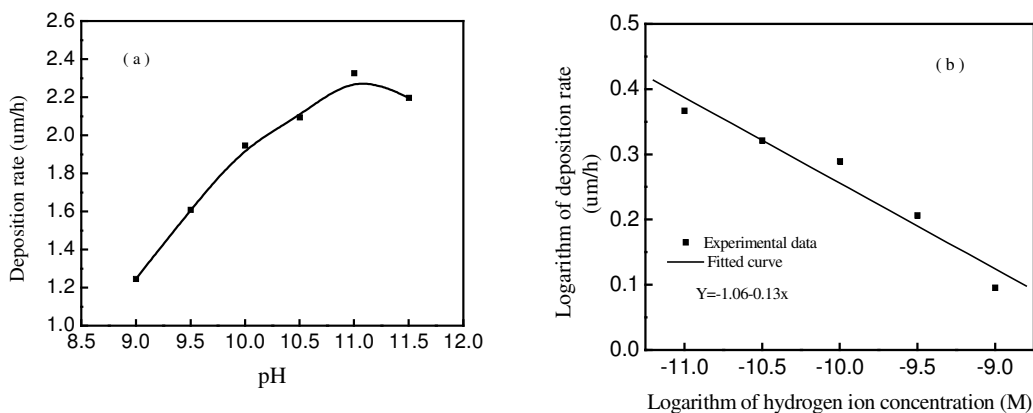


Figure 4. (a) Effect of pH on deposition rate (b) plot of logarithm of deposition rate versus logarithm of hydrogen ion concentration

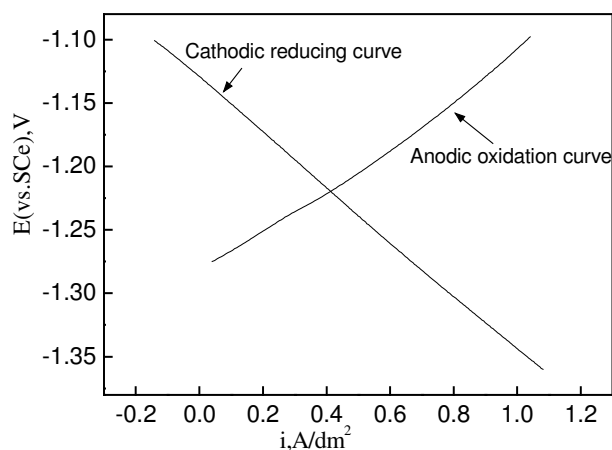


Figure 5. Partial cathodic I-E curve for reduction of Fe^{2+} ions and anodic polarization curve for oxidation of $H_2PO_2^-$

Fig.5 shows the partial cathodic I-E curve for reduction of Fe^{2+} ions and anodic polarization curve for oxidation of $H_2PO_2^-$. The cathodic and anodic curves intersect at one point where the potential and the current being -1.22 V and 0.41 A/dm², respectively, as displayed in Fig.5. According to the mixed potential theory, the deposition reaction was carried out with a current of 0.41 A/dm². The polarization resistance for cathodic and anodic reaction (R_{pc} and R_{pa}) derived from the polarization curves are 4.8 and $5.7\Omega \cdot dm^2$, respectively, which results in the effect of hypophosphite on the

deposition rate is more pronounced than that of FeSO_4 . This consists with the calculation of reaction order and the results of others investigations on the electroless deposition[15,16,30], indicating that the rate-determining step for the chemical iron reduction is the oxidation of hypophosphite.

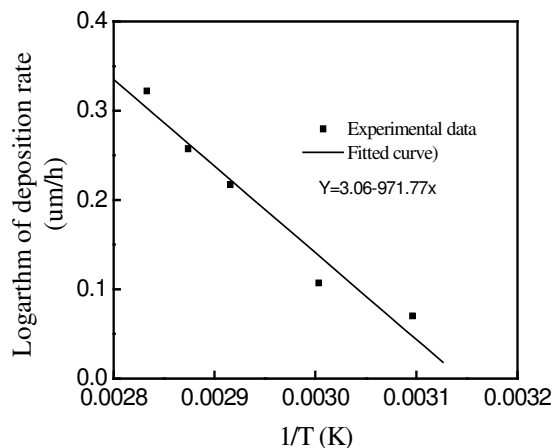


Figure 6. Dependence of the logarithm of deposition rate of Fe-P on inverse temperature

Temperature has an obvious effect on the deposition process. As shown in Fig.1, the Fe-P deposition process may not start below 50°C, the deposition rate increases abruptly with the increase of temperature when the bath temperature is higher than 60 °C. Using the Arrhenius relationship[31], the activation energy, E_a , can be obtained from the slope of the rate of deposition vs reciprocal temperature plot. The data plotted in Fig.6 are representative of the activation energy curves, and from this plot:

$$d \log V / d(1/T) = -E_a / 2.3R$$

and

$$E_a = 18583J / mol$$

4. CONCLUSIONS

The brass substrate is necessary to be connected with aluminum for Fe-P electroless deposition. The connected aluminum provides an active surface and induces the Fe-P electroless deposition due to the reduction of iron cations and the formation of Fe film by currents arising from the local cell composed of the brass substrate as cathode and the connected aluminum foil as anode. The Fe-P film results from a superimposition of the electrochemical process due to the Al dissolution and the chemical process due to the reduction of the Fe cations by H_2PO_2^- anions, accompanied by phosphorus co-deposition and hydrogen evolution. The temperature, concentrations of the metal salt and reducing

agent, and pH of bath influence the behavior of the Fe-P deposition. The activation energy of Fe-P deposition is about 18583 J/mol and the reaction orders of NaH_2PO_2 , FeSO_4 and H^+ are 0.34, 0.18, 0.13, respectively. The effect of hypophosphite on the deposition rate is more pronounced than that of FeSO_4 due to the higher polarization resistance for anodic reaction R_{pa} . This work, together with our and others' recent works, suggests the possibility of future development of electroless Fe-based alloy films with excellent performances.

ACKNOWLEDGEMENTS

The work was financially supported by Hunan Provincial Natural Science Foundation of China(Grant Nos. 06JJ3003 and 05JJ30089).

References

1. A.Kohn, M.Eizenberg, *J.Appl. Phys.* 94(2003)3810
2. A.Kuhn, F.Argoul, J.F.Muzy, et al., *Phys.Rev.Lett.* 73(1994)2998
3. S.L. Wang, *Surf. Coat. Tech.* 186 (2004)372
4. V.M.Dubin, Y.Shacham-Diamand, B.Zhao, et al., *J. Electrochem. Soc.* 144 (1997)898
5. N.M.Hasan, J.J.Mallett, S.G.dos Santos Filho, et al., *Phys.Rev.B* 67(2003)081401(R)
6. J.N. Balaraju, K.S. Rajam, *Surf. Coat. Tech.* 195 (2005) 154
7. L. Magagnin, V. Sirtori, S. Seregni, et al., *Electrochim. Acta* 50 (2005)4621
8. I. Baskaran, T.S.N. Sankara Narayanan, A. Stephen, *Mater. Chem. Phys.* 99(2006) 117
9. T. Osaka, T. Asahi, J. Kawaji, et al., *Electrochim. Acta* 50 (2005) 4576
10. Y. Shacham-Diamand, A. Inberg, Y. Sverdlov, et al., *Electrochim. Acta* 48 (2003) 2987
11. L.B. Li, M.Z. An, G.H. Wu, *Mater. Chem. Phys.* 94(2005)159
12. J.N. Balaraju, C. Anandan and K.S. Rajam, *Appl. Surf. Sci.*, 250(2005) 88
13. N. Petrov, Y. Sverdlov, Y. Shacham-Diamand, *J. Electrochem. Soc.* 149(2002)C187
14. M.E. Touhami, E.Chassaing, M. Cherkaoui, *Electrochim. Acta* 48(2003)3651
15. T. Homma, A.Tamaki, H. Nakai, et al., *J. Electroanal. Chem.* 559(2003)131
16. T. Homma, I. Komatsu, A.Tamaki, et al., *Electrochim. Acta* 47(2001)47
17. S. Shukla, S. Seal, J. Akesson, et al., *Appl. Surf. Sci.* 181(2001) 35
18. C.M. Liu, W.L. Liu, S.H. Hsieh, et al., *Appl. Surf. Sci.* 243(2005) 259
19. Q.L. Rao, G.Bi, Q.H. Lu, et al., *Appl. Surf. Sci.* 240(2005)28
20. A. Maiecki, A. Micek-Ilnicka, *Surf. Coat. Tech.* 123(2000) 72
21. C. Ruscior, E. Croiala, *J. Electrochem. Soc.* 18(1971)696
22. L.L. Wang, L.H. Zhao, G.F. Huang, et al., *Plat. Surf. Finsh.* 88(2001)92
23. L.L. Wang, L.H. Zhao, G.F. Huang, et al., *Z. Metallkd.* 92(2001)391
24. L.L. Wang, W.Q. Huang, G.F. Huang, et al., *Z. Metallkd* 93(2002)298
25. L.L. Wang, L.H. Zhao, G.F. Huang, et al., *Surf. Coat. Tech.* 126(2000) 272
26. B.W. Zhang, W.Y. Hu, D.Q. Zhu, *Physica B* 183(1993)205
27. W.Y. Hu, B.W. Zhang, *Trans. Inst. Metal Finish* 71(1993)30
28. N. Fujita, A. Tanaka, E. Makino, et al., *Appl. Surf. Sci.* 113/114(1997)61
29. G.F. Huang, W.Q. Huang, L.L. Wang, et al., *Electrochim. Acta* 51(2006)4471
30. H.Nakai, T.Homma, I.Komatsu, et al., *J. Phys. Chem. B* 105(2001)1701
31. G.O. Mallory, V.A. Lloyd, *Plat. Surf. Finish.* 72(1985)52